2023 IEEE/ASME International Conference on Advanced Intelligent Mechatronics (AIM)
June 28-30, 2023. Seattle, Washington, USA

Development of Orthopedic Haptic Drill for Spinal Surgery with Penetration Detection Scheme based on Viscosity Estimation

Shunya Takano, *Member, IEEE*. Tomoyuki Shimono, *Senior Member, IEEE*. Takuya Matsunaga, *Member, IEEE*. Mitsuru Yagi, Kouhei Ohnishi, *Life Fellow, IEEE*. Masaya Nakamura, Yuichiro Mima, Kento Yamanouchi, and Go Ikeda.

***Abstract*— In orthopedic surgery, making an incision into the spine involves a risk of injury to the spinal cord. In addition, surgeons must determine penetration into the bone using only their haptic senses. This imposes a heavy burden on the surgeon. In this study, an orthopedic haptic drill with a penetration detection scheme based on viscosity estimation is proposed. This drill detects penetration by monitoring changes in the position and force of the linear motor in the drill. The threshold values are automatically optimized according to the estimated viscosity of the object being cut. Therefore, the proposed drill does not require prior setup of the parameters in accordance with the object being cut. The utility of the proposed drill is verified experimentally.**

I. Introduction

In orthopedic surgery, bone cutting and drilling are common procedures. In spinal surgery, surgeons must cut the spine without damaging the spinal cord. Otherwise, it may result in serious sequela due to any injury to the spinal cord [1], [2]. Moreover, surgeons must determine the penetration of the bone using only their haptic senses. Therefore, surgeons conducting spinal surgery must have significant skill and experience [3]. This is quite burdensome for the surgeon.

Therefore, the development of a new safe orthopedic drill is required. Currently, some studies have been conducted on new drills that stop automatically upon penetrating the bone. Osa *et al.* developed a drill to detect penetration by monitoring the cutting resistance of the drill bit [4], [5]. Lee *et al.* developed a drill to detect penetration by monitoring the force of the load cell and the torque of the rotary motor [6], [7]. Lin *et al.* suggested an algorithm with wavelet transformation of force information to accurately determine the amount of penetration during drilling [8]. Aziz *et al.* monitored the change in the thrust force and position of a robot arm for detection [9]. Dai *et al.* identified the drilling state by using acceleration sensor and laser displacement sensor [10]–[12]. However, these studies require the setup of penetration parameters before cutting the bone or estimating the threshold from the first penetration. Moreover, some studies involved cutting bone using a robot. Thus, they differ from conventional surgeries.

In previous research, a new orthopedic haptic drill was developed [13], [14]. This drill determined penetration by monitoring the change in the position and force of the linear motor in the drill. When the drill detects penetration, the linear motor pulls the drill bit to prevent damage to the spinal cord. In addition, the drill can be operated by a surgeon. Therefore, this drill is applicable to conventional surgeries. The differential values of the position and reaction force of the linear motor are used to detect penetration. These values are suddenly increased or decreased at the penetration. Thus, the drill determined as penetration when two values exceed the threshold values at the same time. However, this method requires the setup of threshold value according to the object being cut. Therefore, an improvement in the algorithm for detecting penetration is required.

This paper proposes an orthopedic haptic drill with a penetration detection scheme based on viscosity. This drill detects penetration by monitoring the changes in position and force. The threshold values are automatically optimized according to the estimated viscosity of the object being cut. Viscosity is estimated using the position and force information of the linear motor in the drill. Therefore, the proposed drill does not require the prior setup of any parameter in accordance with the object being cut. After the drill detects penetration, the drill bit gets pulled into the body of the drill and stops automatically. Therefore, spinal surgeries can be performed in a conventional and safe manner.

The remainder of this paper is organized as follows. In Section II, the structure of the proposed drill is presented. Section III describes the methods of control and penetration detection. In Section IV, the confirmation of the proposed method using bone models is described. Section V presents

Shunya Takano is with the Kanagawa Institute of Industrial Science and Technology, Kawasaki, Kanagawa 210-0821, Japan, and also with the Graduate School of Engineering Science, Yokohama National University, Yokohama 240-8501, Japan (e-mail: sp-takano@res-kistec.jp).

Tomoyuki Shimono is with the Faculty of Engineering, Yokohama National University, Yokohama 240-8501, Japan, and also with the Kanagawa Institute of Industrial Science and Technology, Kawasaki, Kanagawa 210-0821, Japan (e-mail: shimono-tomoyuki-hc@ynu.ac.jp).

Takuya Matsunaga is with the Kanagawa Institute of Industrial Science and Technology, Kawasaki, Kanagawa 210-0821, Japan (e-mail: sp-matsunaga@res-kistec.jp).

Mitsuru Yagi is with Department of Orthopedic Surgery, International University of Health and Welfare, School of Medicine, Narita, Chiba 286-8520, Japan. (e-mail: yagiman@gmail.com).

Kouhei Ohnishi is with the Haptics Research Center, Keio University, Kawasaki, Kanagawa 233-8522, Japan, and also with the Kanagawa Institute of Industrial Science and Technology, Kawasaki, Kanagawa 210-0821, Japan (e-mail: ohnishi@sd.keio.ac.jp).

Masaya Nakamura, Yuichiro Mima, and Kento Yamanouchi are with Department of Orthopedic Surgery, Keio University School of Medicine, Shinjuku-ku, Tokyo 160-8582, Japan (e-mail: masa@keio.jp; mimatschi@yahoo.co.jp; yamaken0331@gmail.com).

Go Ikeda is with the Japan Medtronic Company, Ltd., Minato-ku, Tokyo 108-0075, Japan (e-mail: go.ikeda@medtronic.com).

978-1-6654-7633-1/23/$31.00 ©2023 IEEE

Fig. 1. Proposed orthopedic haptic drill

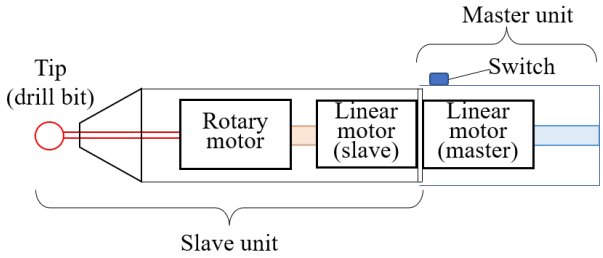

Fig. 2. Schematic of proposed orthopedic haptic drill

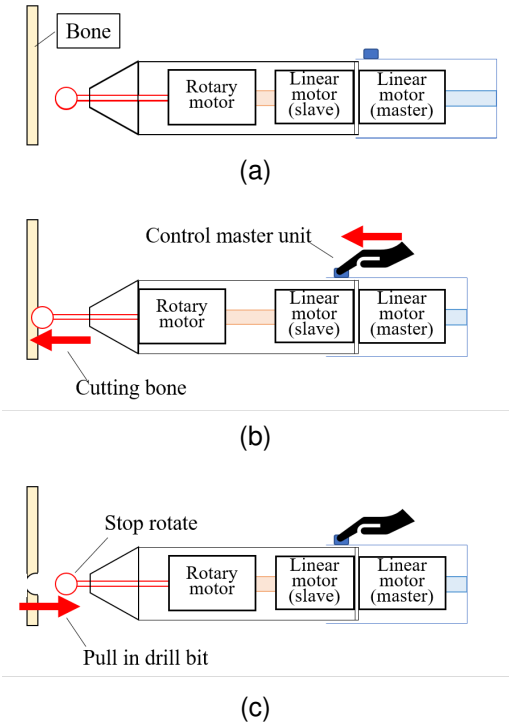

Fig. 3. Schematics of each operation. (a) Conventional state. (b) Bilateral operation. (c) Automatic stop after penetration.

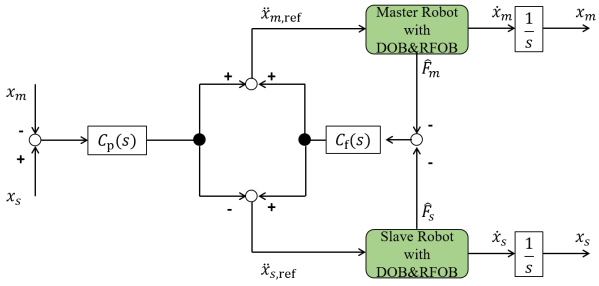

Fig. 4. Block diagram of bilateral control

the results of the animal experiment. Finally, the paper is concluded in Section VI.

II. Structure of Orthopedic Haptic Drill

Fig. 1 shows the structure of the proposed orthopedic haptic drill, and Fig. 2 shows the schematic diagram of the drill. The proposed drill consists of two linear motors with optical encoders and one rotary motor with a rotary encoder. The linear motor is a voice coil motor (Akribis AVM30-15) and the rotary motor is a brushless DC motor (Orbray BMS16-4202BOD). The rotary and linear motors are located in the slave unit of the proposed drill. The rotary motor is mounted on the mover part of the linear motor. Therefore, the slave unit can realize rotary and linear motions of the drill bit. The other linear motor is located in the master unit of the proposed drill. The mover part of the linear motor is connected to the cover part. Additionally, the switch used to control the rotary motor is attached to the cover. The surgeon handles the master unit during surgery.

Fig. 3(a)–(c) presents the schematics of each operation. The drill bit rotates when the surgeon pushes the switch on. During the cutting operation, bilateral control is applied to the two linear motors. Therefore, the drill bit moves synchronously with the master unit (Fig. 3(b)). Thus, the surgeon can cut the bone by controlling the master unit and the switch. When the drill detects penetration, position control is applied to the linear motor on the slave unit to retract the drill bit. In addition, the drill bit automatically stops rotating even when the switch is on (Fig. 3(c)). Therefore, the proposed drill can prevent damage to the spinal cord.

III. Control Method

The proposed orthopedic haptic drill is based on robust acceleration control with a disturbance observer (DOB) and reaction force observer (RFOB) [15] [16]. Proportional velocity control was applied to the rotary motor. The control of the two linear motors was activated based on the operation phase.

A. Gravity compensation

Before starting the operation of the drill, gravity was measured. An orthopedic drill is generally held in the vertical direction. Thus, gravity compensation is required to prevent the linear motor from dropping.

Position control is applied to the two linear motors to estimate the gravity. First, the master and slave units are pulled up by 1 mm using linear motors. Subsequently, this position is maintained for 2 s and the disturbance force is measured by the DOB. The gravitational force is estimated by calculating the average value of the disturbance force. The estimated gravity force $\hat{F}_{\mathrm{gravity}}$ is used as gravity compensation in the RFOB.

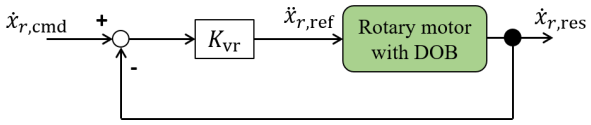

Fig. 5. Block diagram of velocity control

B. Manual Operation

In manual operation, bilateral control is applied to the two linear motors. Fig. 4 shows the block diagram of the bilateral control. The subscripts m and s denote the linear motors in the master and slave units, respectively. x, $\dot{x}$, and $\ddot{x}_{\mathrm{ref}}$ are the position, velocity, and acceleration references, respectively. The linear encoder is used to measure the position. $\hat{F}$, $C_{\mathrm{p}}(s)$, and $C_{\mathrm{f}}(s)$ are the estimated reaction force, position controller, and force controller, respectively. These controllers are given by (1) and (2).

$$C_{\mathrm{p}}(s) = K_{\mathrm{p}} + K_{\mathrm{v}}\frac{sg_{\mathrm{diff}}}{s+g_{\mathrm{diff}}} \quad (1)$$

$$C_{\mathrm{f}}(s) = K_{\mathrm{f}} \quad (2)$$

K_{p}, K_{v}, K_{f}, and g_{diff} are position gain, velocity gain, force gain, and cutoff frequency of pseudo differential, respectively. Bilateral control realizes equations (3) and (4).

$$x_m - x_s = 0 \quad (3)$$

$$F_m + F_s = 0 \quad (4)$$

These equations represent the law of action and reaction. Bilateral control realizes the transmission of haptic sensation between the two linear motors. Thus, the surgeon can feel the reaction force from the drill bit while operating the master unit.

Fig. 5 shows the block diagram of the application of velocity control to the rotary motor. $\dot{x}_{r,\mathrm{cmd}}$, $\dot{x}_{r,\mathrm{res}}$, and K_{vr} are the velocity command, response, and gain of the rotary motor, respectively. The rotary motor is rotated when the surgeon pushes the switch on. In contrast, the rotary motor stops when the switch is off or the drill detects penetration. Thus, when the velocity command is set to 30000 rpm, $\dot{x}_{\mathrm{r,cmd}}$ is defined as (5).

$$\dot{x}_{\mathrm{r,cmd}} = \begin{cases} 1000\pi\,[\mathrm{rad/s}]\,(\text{switch on}) \\ 0\ (\text{switch off or detect penetration}) \end{cases} \quad (5)$$

C. Penetration Detection Scheme

The differential values of the position and reaction force of the linear motor on the slave unit were used to detect the penetration [13]. The reaction force from the bone is applied to the linear motor on the slave unit while cutting the bone. However, the reaction force suddenly decreases when the drill penetrates the bone. In addition, the velocity of the linear motor increases owing to a decrease in the reaction force. Therefore, the differential of the position and reaction force peaks at the penetration. Thus, the drill detects penetration when (6) and (7) are satisfied.

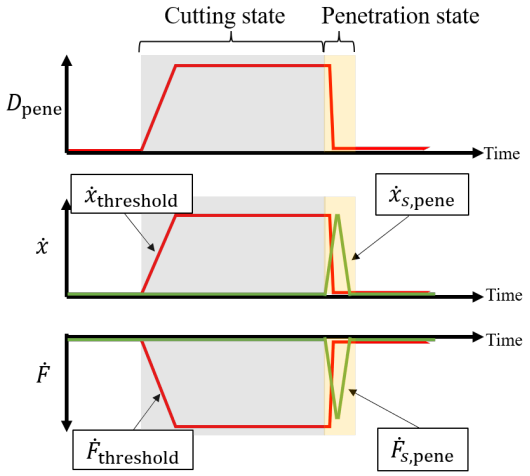

Fig. 6. Transition graph of threshold and viscosity

$$\dot{x}_{s,\mathrm{pene}} > \dot{x}_{\mathrm{threshold}} \quad (6)$$

$$\dot{F}_{s,\mathrm{pene}} < \dot{F}_{\mathrm{threshold}} \quad (7)$$

$\dot{x}_{s,\mathrm{pene}}$ and $\dot{F}_{s,\mathrm{pene}}$ are the velocity and differential value of the reaction force at the linear motor on the slave unit, respectively. $\dot{x}_{\mathrm{threshold}}$ and $\dot{F}_{\mathrm{threshold}}$ are the threshold values. $\dot{x}_{s,\mathrm{pene}}$ and $\dot{F}_{s,\mathrm{pene}}$ are estimated using (8) and (9), respectively.

$$\dot{x}_{s,\mathrm{pene}} = \frac{sg_{\mathrm{pene}}}{s+g_{\mathrm{pene}}}x_s \quad (8)$$

$$\dot{F}_{s,\mathrm{pene}} = \frac{sg_{\mathrm{pene}}}{s+g_{\mathrm{pene}}}\hat{F}_s \quad (9)$$

g_{pene} is the cutoff frequency of the pseudo differential to eliminate the high frequency noise.

In previous research, the threshold values were set at a constant value. However, the peak values of $\dot{x}_{s,\mathrm{pene}}$ and $\dot{F}_{s,\mathrm{pene}}$ were affected by the impedance of the object. For example, the peak value of $\dot{F}_{s,\mathrm{pene}}$ was small when the drill penetrated a soft object. However, the peak value of the penetration signals was larger when the surgeon operated the drill rapidly or applied a large thrust force. Therefore, the peak value of the penetration signal changes according to the surgeon's operation, even for the same object. Hence, the threshold value must be changed according to the object being cut.

The viscosity is used to obtain the characteristics of the cutting object. The velocity and reaction force of the linear motor are used to estimate the viscosity D_{pene} using (10) and (11).

$$D_{\mathrm{pene}} = \frac{\hat{F}_{s,\mathrm{LPF}}}{\dot{x}_{s,\mathrm{pene}}} \quad (10)$$

$$\hat{F}_{s,\mathrm{LPF}} = \frac{g_{\mathrm{pene}}}{s+g_{\mathrm{pene}}}\hat{F}_s \quad (11)$$

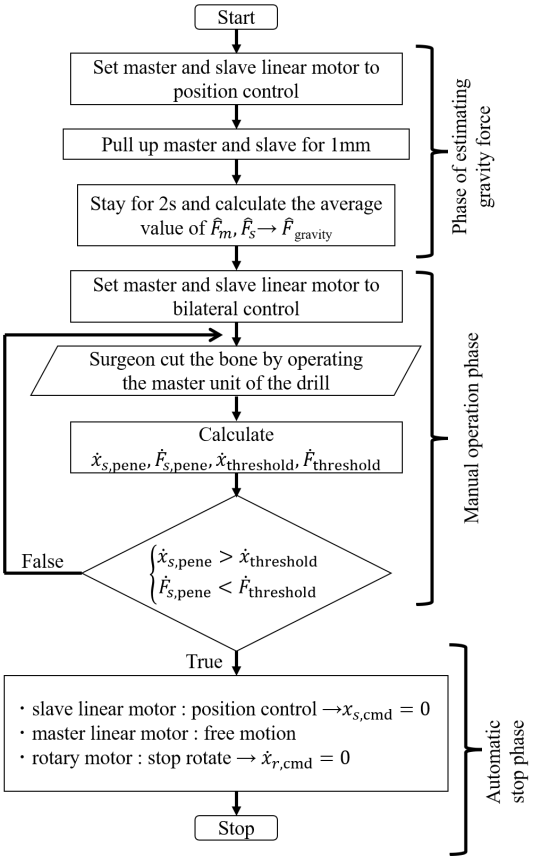

Fig. 7. Flowchart of control method.

In fact, the contact area between the drill bit and cutting object is required to estimate the actual viscosity. However, the contact area cannot be accurately determined because the drill moves along the surface of the bone during spinal surgery. Thus, the viscosity is determined by the velocity and reaction force of the linear motor. Using D_{pene}, the threshold values are determined as (12) and (13).

$$\dot{x}_{\text{threshold}} = \alpha D_{\text{pene}} \tag{12}$$

$$\dot{F}_{\text{threshold}} = \beta D_{\text{pene}} \tag{13}$$

α and β are proportional constant. α and β are determined experimentally based on the inertia and the friction of the drill. Generally, a small reaction force and high velocity occur when cutting soft objects. Thus, the viscosity D_{pene} is estimated as a small value. Therefore, the threshold values are estimated to be small when the drill cuts a soft object. The threshold value can be changed automatically according to the object being cut.

Fig. 6 shows the transition of viscosity and threshold values. During cutting, the reaction force from the object increases, and the velocity, i.e., the cutting speed, decreases. Thus, the threshold value increases when the object is being cut. In contrast, when the drill penetrates the object, the reaction force decreases, and the velocity increases. Thus, the threshold value decreases. However, $\dot{x}_{s,\text{pene}}$ and $\dot{F}_{s,\text{pene}}$ increase with penetration. Therefore, the penetration signals and threshold value crosses each other at penetration. Thus, the drill detects the penetration by satisfying (6) and (7).

After the drill detects penetration, the linear motor on the slave unit is employed as a position control to pull in the drill bit. In addition, the velocity command $\dot{x}_{r,\text{cmd}}$ is set to zero to stop the rotation of the drill bit. The flowchart of the control method is shown in Fig. 7.

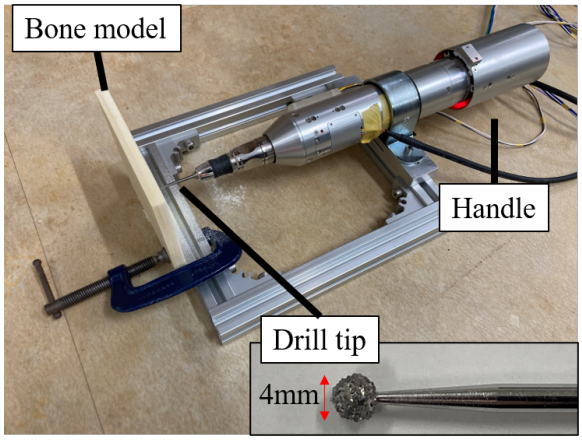

Fig. 8. Experimental setup for cutting bone model

TABLE I
DENSITY OF BONE MODELS

Bone model	Density [kg/m^3]	
	Cortical bone	Cancellous bone
40-20	560.8±56.2	320.4±31.8
30-15	480.5±48.0	240.0±24.0
20-10	320.4±31.8	160.0±16.0

TABLE II
CONTROL PARAMETERS

Parameter	Variable	Value
Sampling time [s]	Δt	0.4×10^{-3}
Position gain [s^{-1}]	K_{P}	6400
Velocity gain (linear motor) [s^{-2}]	K_{V}	160
Velocity gain (rotary motor) [s^{-2}]	K_{Vr}	200
Force gain	K_{F}	1
Rotation speed [rpm]	$\dot{x}_{r,\text{cmd}}$	30000
Cutoff frequency of DOB and RFOB [Hz]	g_{dis}	150
Cutoff frequency of pseudo differential [Hz]	g_{diff}	300
Cutoff frequency of pseudo differential for estimated penetration signals [Hz]	g_{pene}	30
Proportional constant for estimated $\dot{x}_{\text{threshold}}$	α	1.5×10^{-5}
Proportional constant for estimated $\dot{F}_{\text{threshold}}$	β	-1.5×10^{-3}

IV. EXPERIMENTAL VERIFICATION USING BONE MODEL

This section describes the verification of penetration detection using viscosity estimation. Three types of bone model with different impedance values were used.

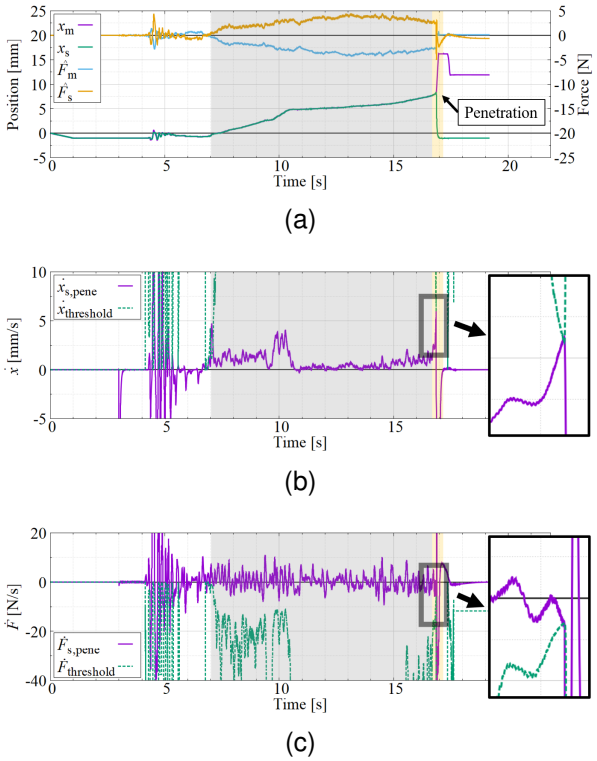

Fig. 9. Results of cutting bone model 20-10 using estimated viscosity. (a) Position and force responses. (b) Differential value of position. (c) Differential value of force.

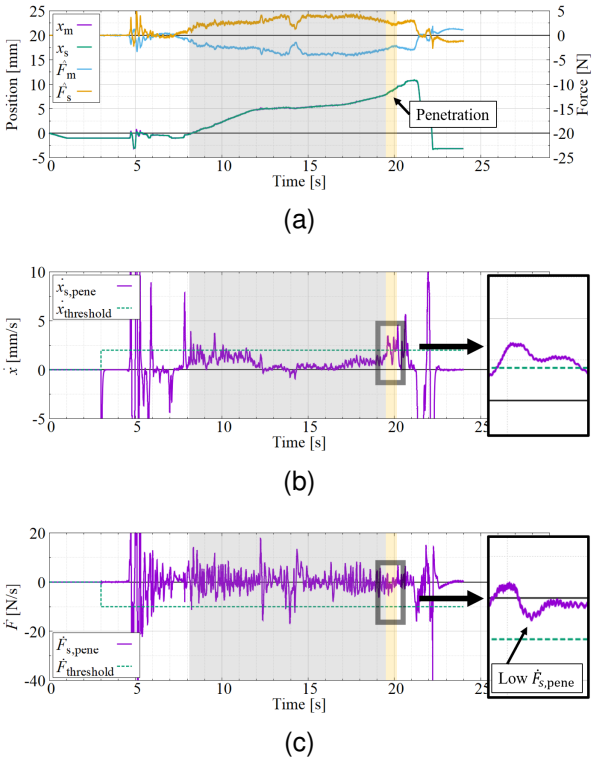

Fig. 10. Results of cutting bone model 20-10 by constant threshold. (a) Position and force responses. (b) Differential value of position. (c) Differential value of force.

TABLE III

EXPERIMENTAL RESULTS OF DRILLING BONE MODELS

		Number of detecting penetrations	
Bone model	Trial	Threshold from estimated viscosity (Proposed method)	Constant threshold (Previous method)
40-20	3	3 (100%)	3 (100%)
30-15	3	3 (100%)	1 (33.3%)
20-10	3	3 (100%)	1 (33.3%)

Table I lists the densities of the bone models. The bone models were made of rigid polyurethane foam and constructed using two layers: the cortical bone layer and the cancellous bone layer. The number of bone models represents the grade of pounds per cubic foot (PCF). Therefore, a higher value represents a higher stiffness. The stiffness of the bone model 40-20 is equivalent to the human bone. The bone model 30-15 and 20-10 imitate the stiffness of osteoporosis's bone. The thickness of the bone model was 3 mm for the cortical bone layer and 5 mm for the cancellous bone layer.

A. Experimental setup

Fig. 8 shows the experimental setup for cutting the bone model. The proposed drill and bone model were fixed in an aluminum frame. The surgeon moved the drill bit vertically toward the bone model by moving the master unit. A diamond bar (Medtronic 10BA40DC) was used as the drill bit. The surgeon cuts each bone model three times. Table II shows the parameters of the controller. The verification of detecting penetration by the proposed method was conducted.

Additionally, the same experiment was conducted by using the previous method for comparison. The constant threshold values $\dot{F}_{\mathrm{threshold}} = -10.0$ and $\dot{x}_{\mathrm{threshold}} = 2.0$ were used as the previous method. The values were determined based on the stiffness of the bone model 40-20.

B. Experimental result

Table III lists the experimental results for penetration detection in each bone model. The results show that the proposed method detects the penetration in every bone model. In contrast, penetration could not be detected using a constant threshold value in the model with 30-15 and 20-10. This is because the threshold values were set based on the bone model 40-20. Thus, penetration signal $\dot{F}_{s,\mathrm{pene}}$ could not reach the threshold value in the model with lower stiffness.

Fig. 9 and 10 show the experimental results of drilling the bone model 20-10 by the proposed method and previous method, respectively. The gray shaded area represents the cutting of the bone model, and the yellow shaded area represents the drill penetrating the bone model.

In Fig. 9(a), the master and slave units were operated simultaneously while cutting the bone model. Furthermore, the slave unit was rapidly changed to -2 mm at approximately 17 sec, when the penetration signals and threshold values crossed each other (Fig. 9(b),(c)). Thus, the proposed method detected penetration and stopped automatically by pulled in the drill

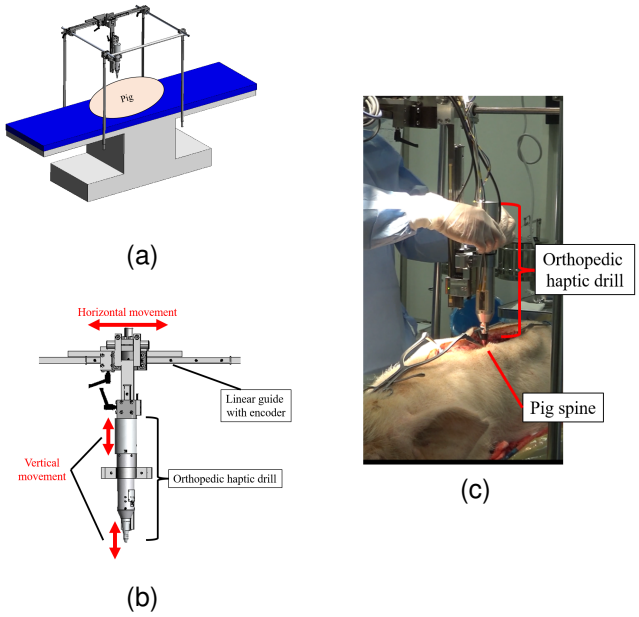

Fig. 11. Experimental setup of animal experiment. (a) General view of setup. (b) Setup around drill. (c) Intraoperative view of animal experiment.

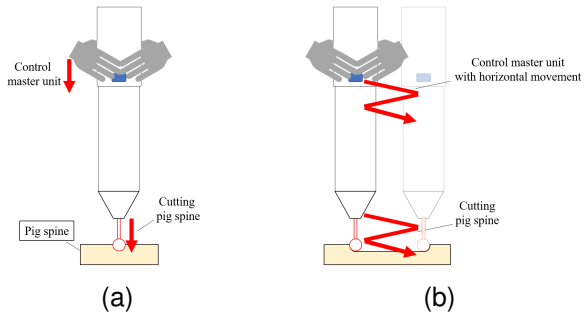

Fig. 12. Schematics of operation in experiment. (a) Vertical cutting. (b) Horizontal cutting.

TABLE IV
EXPERIMENTAL RESULT OF CUTTING PIG SPINE

Surgeon	Trial	Number of detecting penetrations
A	3	3 (100%)
B	3	3 (100%)
C	3	3 (100%)

bit at approximately 8 mm. This distance corresponds to the thickness of the bone model. Therefore, the proposed method correctly detected penetration.

In contrast, the previous method could not detect penetration because of the low $\dot{F}_{s,\mathrm{pene}}$ (Fig. 10(c)). The previous method used constant threshold values in the experiment. Therefore, $\dot{F}_{s,\mathrm{pene}}$ could not reach the threshold value due to the low stiffness. Thus, the setup of threshold value was needed in the previous method. However, in Fig. 9(c), $\dot{F}_{\mathrm{threshold}}$ is decreased when penetrating the bone model. Therefore, the proposed method optimizes the threshold value according to the impedance of the cutting object. Thus, the efficacy of the proposed method was verified.

V. ANIMAL EXPERIMENT

We verified the proposed method using animal experiments. Pig spines were used in this experiment. Animal experiments were approved by the Judging Committee of Experimental Animal Ethics of Keio University School of Medicine (authorization number:18047). All animals were purchased from Kagoshima Miniature Swine Research Center, Kagoshima, Japan. The animals were housed and treated according to the rules approved by the Ethics Committee.

A. Experimental setup

Fig. 11(a) shows the experimental setup of the animal experiment. The drill was fixed above the pig spine using an aluminum frame and pipes. Frames were used to mitigate the effects of hand vibrations. In addition, the linear guide and encoder were attached to the frame (Fig. 11(b)). Therefore, horizontal movement can be measured. The control parameters shown in Table II were used in this experiment.

The verification of penetration detection by different surgeon was conducted. Three surgeons conducted the experiment individually. The surgeon cuts the spine vertically using the master unit of the drill (Fig. 12(a)). After the drill detected penetration and stopped automatically, the surgeon visually checked the hole. If the hole penetrated the spine and the spinal cord was not damaged, the penetration detection of the drill was considered to be a success. Each surgeon drilled the spine three times.

B. Experimental result

Table. IV shows the result of animal experiment. From the results, the proposed drill detected penetration in every trial performed by each surgeon. Therefore, it is certain that the proposed method optimizes the threshold value based on the surgeon's operation. Therefore, the validity of the proposed method was verified.

C. Horizontal cutting

In actual spinal surgery, the surgeon moves the drill horizontally along the surface of the spine to create a large hole. Thus, the detection of penetration with a horizontal movement was also confirmed. The surgeon moved the drill horizontally by sliding it along the linear guide (Fig. 12(b)).

Fig. 13 shows the transition of the drill bit in the operation. The color of the line is related to the time of experiment. From the results, the surgeons cut the spine by moving the drill horizontally. When the drill made an incision into the spine approximately 7 mm deep, it detected the penetration and stopped automatically by pulled in the drill bit. Visual observation revealed that the hole penetrated the spine and the spinal cord was not damaged. Therefore, the proposed method was valid for horizontal drilling as well.

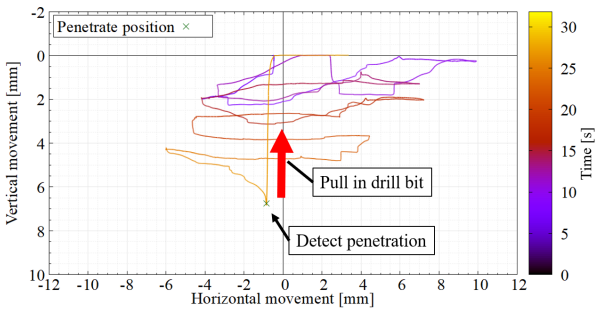

Fig. 13. Experimental result of drilling with horizontal movement. (Surgeon A)

VI. Conclusion

This study proposes an orthopedic haptic drill with a penetration-detection scheme. The drill automatically detects penetration and stops to prevent damage to the spinal cord. Penetration was detected by monitoring the differential values of the position and reaction force of the linear motor. Viscosity estimation was applied to the detection scheme. Thus, the proposed drill optimizes the threshold value based on the impedance of the object being cut. Therefore, the drill can detect penetration without manual adjustment of the threshold value. Three types of bone models were used in the experiment to verify the proposed drill. The proposed drill detected penetration in every bone model. In addition, an animal experiment was conducted by three surgeons. The proposed drill detected the penetration during experimental verification by every surgeon. Therefore, the proposed orthopedic haptic drill can be utilized to detect penetration of the spine.

However, pose estimation of the drill is required in future work. Experiments were conducted by fixing the drill to maintain it in the same posture. This is because the value of gravity compensation corresponds only to the initial posture. However, the drill posture is not constant during spinal surgery. Therefore, pose estimation is required to realize precise control.

Additionally, miniaturization of the proposed drill is required. The drill is too large to be held in the hand because it includes linear motors. Therefore, design optimization will be conducted in future studies.

Acknowledgment

This research was supported by AMED under Grant Number JP22he2202014.

References

[1] P. Guerin, A. Benchikh., E. Fegoun, I. Obeid, O. Gille, L. Lelong, S. Luc, A. Bourghli, J. C. Cursolle, V. Pointillart, and J. Vital, "Incidental durotomy during spine surgery: Incidence, management and complications. A retrospective review," *Injury*, vol. 43, issue 4, pp. 397–401, 2012.

[2] Y. R. Rampersaud, E. R. P. Moro, M. A. Neary, K. White, S. J. Lewis, E. M. Massicotte, and M. G. Fehlings, "Intraoperative Adverse Events and Related Postoperative Complications in Spine Surgery: Implications for Enhancing Patient Safety Founded on Evidence-Based Protocols," *Spine*, vol. 31, no. 13, pp. 1503–1510, June 2006.

[3] Y. Imajo, T. Taguchi, K. Yone, A. Okawa, K. Otani, T. Ogata, H. Ozawa, Y. Shimada, M. Neo, and T. Iguchi, "Japanese 2011 nationwide survey on complications from spine surgery," *Journal of Orthopaedic Science*, vol. 20, issue 1, pp. 38-54, 2015.

[4] T. Osa, C. F. Abawi, N. Sugita, H. Chikuda, S. Sugita, H. Ito, T. Moro, Y. Takatori, S. Tanaka, and M. Mitsuishi, "Autonomous penetration detection for bone cutting tool using demonstration-based learning," *2014 IEEE International Conference on Robotics and Automation (ICRA)*, pp. 290–296, 2014.

[5] T. Osa, C. F. Abawi, N. Sugita, H. Chikuda, S. Sugita, T. Tanaka, H. Oshima, T. Moro, S. Tanaka, and M. Mitsuishi, "Hand-Held Bone Cutting Tool With Autonomous Penetration Detection for Spinal Surgery," *IEEE/ASME Transactions on Mechatronics*, vol. 20, no. 6, pp. 3018–3027, Dec. 2015.

[6] W. Lee, C. Shih, and S. Lee, "Force control and breakthrough detection of a bone-drilling system," *IEEE/ASME Transactions on Mechatronics*, vol. 9, no. 1, pp. 20–29, Mar. 2004.

[7] W. Lee, and C. Shih, "Control and breakthrough detection of a three-axis robotic bone drilling system," *Mechatronics*, vol. 16, issue 2, pp. 73–84, 2006.

[8] L. Qi and M. Q.-H. Meng, "Real-time break-through detection of bone drilling based on wavelet transform for robot assisted orthopaedic surgery," *2014 IEEE International Conference on Robotics and Biomimetics (ROBIO 2014)*, pp. 601–606, 2014.

[9] M. H. Aziz, M. A. Ayub, and R. Jaafar, "Real-time Algorithm for Detection of Breakthrough Bone Drilling," *Procedia Engineering*, vol. 41, pp. 352–359, 2012.

[10] Y. Dai, Y. Xue, and J. Zhang, "Vibration-Based Milling Condition Monitoring in Robot-Assisted Spine Surgery," *IEEE/ASME Transactions on Mechatronics*, vol. 20, no. 6, pp. 3028–3039, Dec. 2015.

[11] Y. Dai, Y. Xue, and J. Zhang, "Milling State Identification Based on Vibration Sense of a Robotic Surgical System," *IEEE Transactions on Industrial Electronics*, vol. 63, no. 10, pp. 6184–6193, Oct. 2016.

[12] Y. Dai, Y. Xue, and J. Zhang, "Bioinspired Integration of Auditory and Haptic Perception in Bone Milling Surgery," *IEEE/ASME Transactions on Mechatronics*, vol. 23, no. 2, pp. 614–623, Apr. 2018.

[13] H. Kobayashi, T. Matsunaga, H. Asai, S. Takano, T. Shimono, M. Yagi, K. Ohnishi, and M. Nakamura, "Development of Orthopedic Haptic Drill for Detection of Penetration," *The7th IEEJ International Workshop on Sensing, Actuation, Motion Control, and Optimization (SAMCON2021)*, Mar. 2021.

[14] K. Yamanouchi, S. Takano, Y. Mima, T. Matsunaga, K. Ohnishi, M. Matsumoto, M. Nakamura, T. Shimono, and M. Yagi, "Validation of a surgical drill with a haptic interface in spine surgery," *Scientific Reports*, vol. 13, Jan. 2023.

[15] K. Ohnishi, M. Shibata, and T. Murakami, "Motion control for advanced mechatronics," *IEEE/ASME Transactions on Mechatronics*, vol. 1, no. 1, pp. 56–67, Mar. 1996.

[16] T. Murakami, F. Yu, and K. Ohnishi, "Torque sensorless control in multidegree-of-freedom manipulator," *IEEE Transactions on Industrial Electronics*, vol. 40, no. 2, pp. 259–265, Apr. 1993.